Microchimica Acta (2020) 187: 110
https://doi.org/10.1007/s00604-019-3897-4

ORIGINAL PAPER

Colorimetric determination of ascorbic acid using a polyallylamine-stabilized IrO_2/graphene oxide nanozyme as a peroxidase mimic

Huiyuan Sun[1,2] · Xueliang Liu[1] · Xinhuan Wang[1] · Qiusen Han[1,3] · Cui Qi[1] · Yanmei Li[2] · Chen Wang[1,3] · Yongxiang Chen[2] · Rong Yang[1,3]

Received: 13 May 2019 / Accepted: 6 October 2019 / Published online: 8 January 2020

Abstract

The authors describe a peroxidase-mimicking nanozyme composed of IrO_2 and graphene oxide (GO). It was synthesized from monodisperse IrO_2 nanoparticles with an average diameter of 1.7 ± 0.3 nm that were prepared by pulsed laser ablation in ethanol. The nanoparticles were then placed on polyallylamine-modified GO nanosheets through electrostatic interaction. The peroxidase-like activity of the resulting nanocomposites was evaluated by catalytic oxidation of 3,3′,5,5′-tetramethylbenzidine in the presence of H_2O_2. Kinetic results demonstrated that the catalytic behavior of the nanocomposites follows Michaelis-Menten kinetics. Experiments performed with terephthalic acid and cytochrome C confirmed that the peroxidase-like activity originated from the electron transfer mechanism rather than from generation of hydroxy radicals. The peroxidase-like activity is inhibited in the presence of ascorbic acid (AA). Based on this property, a colorimetric assay was developed for the determination of AA by exploiting the peroxidase-like activity of IrO_2/GO nanocomposites. The linear relationship between absorbance at 652 nm and the concentration of AA was acquired. The limit of detection for AA is 324 nM. Further applications of the method for AA detection in real samples were also successfully demonstrated.

Keywords Pulsed laser ablation · IrO_2/GO nanocomposites · Nanozymes · Nanoprobes · Peroxidase-like activity · Colorimetric detection

Introduction

Ascorbic acid (AA) participates in many physiological and biochemical processes as a cofactor for several enzymes [1, 2]. Insufficient or excessive AA can lead to scurvy and anemia, accompanied by some psychological abnormalities [3]. Therefore, it is important to develop a convenient and rapid method with high selectivity and accuracy for the determination of AA in physiological and clinical diagnosis. Various methods have been developed to detect AA in recent years, including fluorescence [4], ultra-performance liquid chromatography (UPLC) with UV detector [5] and chemiluminescence (CL) [6].

A variety of nanomaterials such as Fe_3O_4 [7], CeO_2 [8, 9], CoOOH [10], noble metal nanoparticles [11–13], metal organic frameworks [14, 15] and carbon nanomaterials [16, 17], which are called artificial enzymes or nanozymes have been reported to exhibit peroxidase-like activity. In the presence of H_2O_2, these nanozymes can catalyze the substrates such as

Huiyuan Sun and Xueliang Liu contributed equally to this work.

Electronic supplementary material The online version of this article (https://doi.org/10.1007/s00604-019-3897-4) contains supplementary material, which is available to authorized users.

✉ Yongxiang Chen
chen-yx@mail.tsinghua.edu.cn

✉ Rong Yang
yangr@nanoctr.cn

1 CAS Key Lab for Biomedical Effects of Nanomaterials and Nanosafety, Center of Materials Science and Optoelectronics Engineering, CAS center for Excellence in Nanoscience, National Center for Nanoscience and Technology, UCAS, Beijing 100190, People's Republic of China

2 Key Laboratory of Bioorganic Phosphorus Chemistry and Chemical Biology (Ministry of Education), Department of Chemistry, Tsinghua University, Beijing 100084, People's Republic of China

3 Sino-Danish College, UCAS, Sino-Danish Center for Education and Research, Beijing 100190, People's Republic of China

3,3′,5,5′-tetramethylbenzidine (TMB), 2,2′-azino-bis(3-ethylbenzthiazoline-6-sulfonic acid) (ABTS) and o-phenylenediamine (OPD) to develop blue, green and orange color, respectively. The peroxidase-like activity of nanomaterials can be adjusted by AA resulting in the color change which can be directly observed visually. Peroxidase-based nanoprobes were reported to determine AA with high sensitivity and selectivity based on the antioxidant properties of AA [18]. Unlike nature enzymes, nanozymes with low cost and high stability can be easily designed and synthesized by physical-chemical methods, which show a promising potential in environmental monitoring and biological analysis.

Chemical method has achieved great success in preparation of nanomaterials. However, chemical reagents such as metal salts, surfactants and solvents are indispensable in the synthesis process, which is not an environmentally friendly way [19, 20]. As an alternative to traditional chemical method, pulsed laser ablation in liquid (PLAL) has drawn much interest in preparation of nanoparticles [21, 22]. Briefly, the dispersion of nanoparticles can be obtained by focusing the pulsed laser beam on the surface of a bulk target immersed in liquid. It has been reported that the PLAL-synthesized nanoparticles tend to be absorbed on supports owing to the surface charge and the absence of surface ligands [23, 24]. However, it's still a challenge for synthesis of homogeneous ultrasmall nanoparticles using PLAL method.

Herein, we report a facile and green method to synthesize IrO_2/GO nanozyme as a peroxidase mimic for the colorimetric detection of AA. The ultrafine IrO_2 nanoparticles with narrow size distribution were prepared by PLAL. To prevent the aggregation, the polyallylamine-modified GO was chosen as the support of IrO_2 due to its remarkable hydrophilicity and high surface area [25]. IrO_2/GO nanocomposites exhibited excellent peroxidase-like activity towards the oxidation of TMB in the presence of H_2O_2. It is the first report to prepare IrO_2/GO nanozyme for colorimetric detection of AA based on the inhibition of peroxidase-like activity of catalyst.

Experimental

Materials

Iridium plate (thickness 2 mm, diameter 12 mm) with purity 99.99% was purchased from China New Metal Materials Technology Co., Ltd. (Beijing, China, https://cnm2188.en.china.cn). Ascorbic acid (AA), graphene oxide (GO) sheets, ethanol, poly(allylamine hydrochloride) (PAH), H_2O_2, dimethylsulfoxide (DMSO), CH_3COOH and $CH_3COONa{\cdot}3H_2O$ were obtained from Aladdin Industrial Corporation (Shanghai, China, https://www.aladdin-e.com). TMB was obtained from J&K Scientific Ltd. (Beijing, China, https://www.jk-scientific.com). Sodium chloride (NaCl), potassium chloride (KCl), calcium chloride ($CaCl_2$), urea, uric acid (UA), glucose, lactose and terephthalic acid (TA) were bought from Sinopharm Chemical Reagent Co., Ltd. (Shanghai, China, https://www.sinoreagent.com). Fructose, maltose monohydrate, glutamic acid (Glu), serine (Ser), lysine (Lys) and phenylalanine (Phe) were bought from Sigma-Aldrich (Shanghai, China, https:// www.sigmaaldrich.com/ china-mainland.html). Reduced cytochrome C (Cyt C) was purchased from Abcam (Shanghai, China, https://www.abcam.cn). Bovine serum albumin (BSA) was purchased from Beijing Jingke Hongda Biotechnology Co., Ltd. (Beijing, China, http://www.jingke.com.cn). The Mizone beverage (20 mg AA per 100 mL) and Vitamin C tablets (420 mg AA per tablet) were bought from local supermarket and pharmacy, respectively. Ultrapure water with a resistivity of 18.25 MΩ·cm was obtained by using a Millipore Ultrapure water system.

Preparation of polyallylamine (PAH)-stabilized IrO_2/GO

The ultrafine IrO_2 colloid was synthesized by laser ablation method. 100 mg PAH was dissolved in 50 mL 1 $mg{\cdot}mL^{-1}$ GO dispersion to get polyallylamine- modified GO dispersion. IrO_2 colloid was mixed with certain amount of modified GO dispersion and incubated at room temperature to obtain IrO_2/GO nanocomposites. The nanocomposites were centrifugalized, dried and redispersed in water for further use. The peroxidase-like catalytic activity of IrO_2/GO nanocomposites was then investigated and the composites were characterized by different techniques. See the supporting material for the detailed procedures.

Catalytic reaction mechanism

To verify whether hydroxyl radicals are involved in the reaction system, TA is employed. As a fluorescence probe, TA can capture hydroxyl radicals in reaction system and generate high fluorescent 2-hydroxy terephthalic acid. Briefly, TA (0.5 mM), H_2O_2 (10 mM) and 10 μL IrO_2/GO were mixed and added into 500 μL acetate buffer (0.1 M, pH = 4.0) and the mixture was incubated at room temperature for 60 min. Subsequently, the fluorescence spectra of the reaction solution at 350–600 nm were recorded by a fluorescence spectrophotometer with an excitation wavelength of 315 nm.

Cyt C was used to verify the electron transfer effect of IrO_2/GO nanocomposites. The reduced Cyt C solution was diluted by acetate buffer (0.1 M, pH = 4.0). 10 μL IrO_2/GO and 50 μL Cyt C were added into 440 μL acetate buffer (0.1 M, pH = 4.0). Then the mixture was incubated at room temperature for 4 h. The control experiment was conducted in the absence of IrO_2/GO nanocomposites. Experiment in hypoxia was also conducted to eliminate the influence of dissolved oxygen.

The buffer was bubbled by N_2 for 30 min and the solution was incubated for 4 h in a nitrogen atmosphere. The absorption spectra of Cyt C were recorded using a UV-vis absorbance spectrometer at 300–800 nm.

Colorimetric determination of ascorbic acid (AA)

The colorimetric detection of AA was performed in the IrO_2/GO–H_2O_2–TMB reaction system. Specifically, 10 μL H_2O_2 (250 mM), 5 μL TMB (50 mM in DMSO), 470 μL acetate buffer (0.1 M, pH = 4.0) and 10 μL different concentrations of AA (final concentrations: 0–70 μM) were mixed in a 1.5 mL tube, then 5 μL IrO_2/GO dispersion was added into the above reaction system. The absorbance variations at 652 nm were recorded by a UV-vis spectrometer after 10 min of the reaction at room temperature.

To investigate the feasibility of the established method for detecting AA in real samples, the colorimetric assay for AA detection was also performed in simulated serum, vitamin C tablets and Mizone beverage. The "serum" was simulated by 5 wt% BSA solutions with different concentrations of AA (1.0 mM, 2.5 mM and 5.0 mM). The vitamin C tablets were dissolved in 40 mL water and filtered by a PTFE syringe filter to make a colloid. The Mizone beverage was ready for detection without further preparations. Then 10 μL simulated serum, vitamin C colloid and Mizone beverage were tested respectively. The detection procedure was the same as mentioned above.

Results and discussion

Choice of materials

IrO_2 nanoparticles have a wide range of applications in hydrogen evolution and oxygen evolution reactions [26], however, their properties in peroxidase mimic activity have rarely been reported. Similarly, PLAL has been mostly studied on the preparation of noble metals such as Au, Pt and Ag [27], the preparation of Ir nanomaterials by PLAL has not been reported yet. Metal Iridium nanoparticles are easily oxidized to form IrO_2 nanoparticles when exposed to air, therefore, the dispersion of IrO_2 nanoparticles can be prepared by pulsed laser ablation of Iridium targets. However, the colloid was unstable and the IrO_2 nanoparticles aggregated, which would significantly reduce the catalytic activity. The IrO_2 nanoparticles were then adsorbed on polyallylamine- modified GO nanosheets and wouldn't aggregate.

Characterization of the IrO_2/GO nanocomposites

The preparation process and peroxidase-like activity of IrO_2/GO nanocomposites are illustrated in Fig. 1. Briefly, the IrO_2 nanodispersion was firstly prepared by pulsed laser ablation in ethanol with assistance of ultrasonication. After polyallylamine modification, the surface charge of GO was changed from negative charge to positive charge. Then a certain amount of modified GO dispersion was mixed with IrO_2 nanodispersion by ultrasonication and incubated at room temperature to obtain the IrO_2/GO nanocomposites. As a typical reaction substrate, TMB was used to evaluate the peroxidase-like activity of IrO_2/GO nanocomposites in the presence of H_2O_2. The deep blue color of oxidized TMB was observed, which demonstrated the high peroxidase-like activity of IrO_2/GO nanocomposites. However, when AA was added, the catalytic oxidation of TMB was inhibited and the color of reaction solution changed from blue to colorless with increasing concentration of AA. Therefore, the IrO_2/GO nanocomposites can be used for colorimetric detection of AA based on the high peroxidase-like activity.

The TEM and HADDF images of IrO_2 nanoparticles and IrO_2/GO nanocomposites are shown in Fig. S1 and Fig. 2. As seen in Fig. S1, the monodisperse and ultrafine IrO_2 nanoparticles were successfully prepared by PLAL. One can see that the ultrafine and highly dispersed IrO_2 nanoparticles were uniformly decorated on the surface of GO nanosheets (Fig. 2b and c) after mixing with the polyallylamine-modified GO dispersion. The HRTEM image of the IrO_2 nanoparticles inserted in Fig. 2b shows that the d-spacing value of 0.224 nm, which refers to the (200) facet of IrO_2 [28]. The average size of IrO_2 nanoparticles was 1.7 ± 0.3 nm by counting more than 200 nanoparticles. The monodisperse IrO_2 nanoparticles on GO indicated that GO had effectively inhibited the aggregation of IrO_2 nanoparticles. There were no unsupported IrO_2 nanoparticles observed, which indicated that the GO was an excellent support.

The driving force for IrO_2 nanoparticles depositing on polyallylamine-modified GO was the electrostatic interaction, which had been confirmed by the results of zeta potential analysis (Fig. S2). In spite of the drastic sonication, the IrO_2 nanoparticles were still uniformly and firmly anchored on the surface of GO nanosheets, which implied a strong interaction between IrO_2 and polyallylamine-modified GO. The concentration of IrO_2/GO was 240.3 $\mu g \cdot mL^{-1}$ with IrO_2 loading 38.2 wt%, which was confirmed by the ICP-OES analysis.

To further confirm the chemical states of IrO_2/GO nanocomposites, the XPS analysis was evaluated. The survey spectra of IrO_2/GO nanocomposites with strong peak intensity of Ir 4d and 4f, C 1 s and O 1 s are presented in Fig. S3. The peaks at 62.2 eV and 65.2 eV in high resolution spectra corresponded to the binding energies of $4f_{7/2}$ and Ir $4f_{5/2}$ of Ir^{4+} (Fig. S3c), respectively [29]. Clearly, there were no peaks of the metallic Ir(0) at 60.8 eV, which confirmed the completely oxidation of IrO_2 after laser ablation [30].

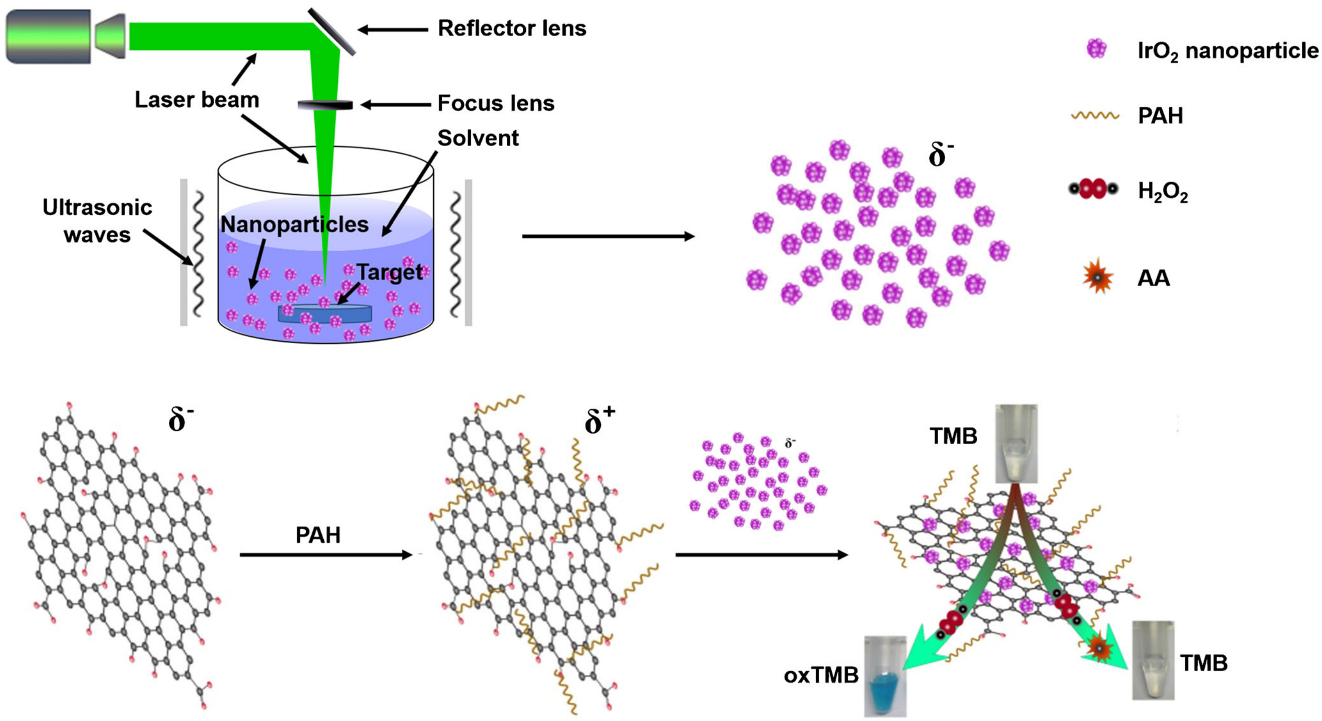

Fig. 1 Schematic illustration of the preparation of PAH stabilized IrO_2/GO nanocomposites and the colorimetric detection of AA based on the peroxidase-like activity of IrO_2/GO nanocomposites

Peroxidase-like activity of IrO_2/GO

In order to investigate the peroxidase-like activity of IrO_2/GO, TMB was chosen as a typical chromogenic substrate in the presence of H_2O_2 at room temperature. The enzymatic activities of GO and IrO_2/GO are presented in Fig. 3, while the buffer and H_2O_2 were employed as negative and positive control, respectively. The blue color and the maximum absorbance at 652 nm of IrO_2/GO–H_2O_2–TMB reaction system suggested the high peroxidase-like activity of IrO_2/GO, while there were no color changes without IrO_2/GO catalyst or H_2O_2 (a, b and d). A faint blue color in the GO system indicated an insignificant peroxidase-like activity of GO compared to IrO_2/GO nanocomposites. The results demonstrated that the color change was attributed to the high peroxidase-like activity of IrO_2/GO nanocomposites.

To get better experimental results, the following parameters were optimized: (a) pH value of buffer; (b) temperature; (c) the concentration of H_2O_2; (d) the dosage of IrO_2/GO catalyst. Respective data and figures are given in the Electronic Supporting Material (Fig. S4–6). The following experimental conditions were found to give best results: (a) Best pH value of buffer: 4; (b) Best temperature value: 55 °C. The catalytic activity was enhanced with increasing concentrations of H_2O_2 and IrO_2/GO. To simplify the experiment, all colorimetric reactions were carried out at room temperature. Therefore, the experiment parameters with pH value of 4.0 and concentrations of TMB 0.5 mM, H_2O_2 5 mM and IrO_2/GO 2.4 μg·mL^{-1} were chosen in the following colorimetric detection assay at room temperature.

Furthermore, the steady-state kinetics of the oxidation process were investigated using the enzyme kinetic model. The kinetic data were obtained by varying the TMB concentrations at a fixed H_2O_2 concentration and vice versa. Typical Michaelis-Menten curves were obtained in a certain concentration range of TMB or H_2O_2 as shown in Fig. 4. The Michaelis-Menten constant (K_m) and the maximum velocity (v_{max}) were obtained from the Lineweaver–Burk double reciprocal plots (Fig. 4b and d). K_m indicates the affinity of an enzyme to its substrate. It is believed that a low K_m value suggests a high affinity [31]. While the K_m of IrO_2/GO nanocomposites towards TMB and H_2O_2 were 0.56 mM and 5.19 mM respectively, which were both slightly higher than horseradish peroxidase (HRP, 0.434 mM to TMB and 3.70 mM to H_2O_2) (Table S1) [8]. Compared to HRP, the similar K_m values and high v_{max} values of IrO_2/GO nanocomposites indicated that IrO_2/GO was a highly potential candidate for colorimetric assays based on the peroxidase-like activity.

Furthermore, the mechanism of peroxidase-like activity of IrO_2/GO nanocomposites was investigated. It has been reported that the peroxidase-like activity of nanozymes can be ascribed to the generation of hydroxyl radical and the electron transfer process. To clarify the catalytic mechanism of IrO_2/GO nanocomposites, terephthalic acid (TA), a fluorescence probe for hydroxyl radical, was used to check the production

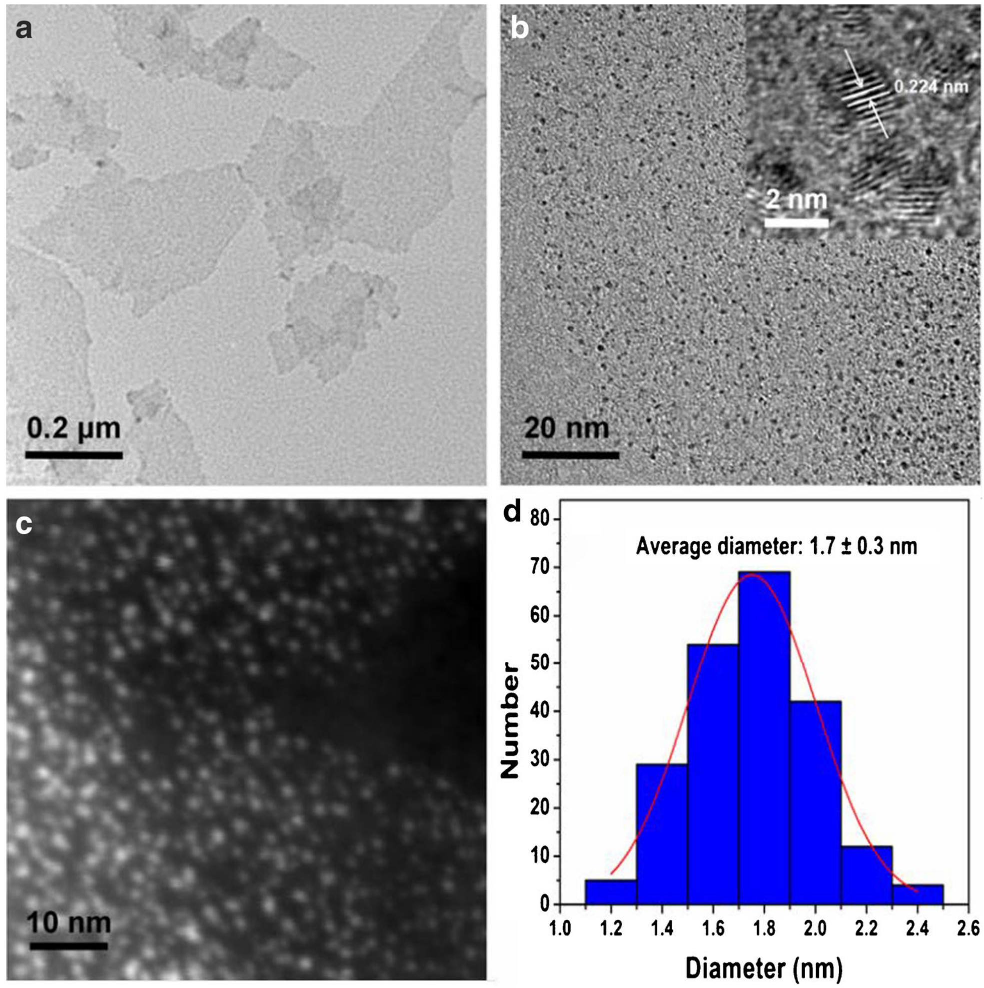

Fig. 2 (a) and (b) TEM images of IrO_2/GO nanocomposites, inset: the HRTEM image; (c) the HAADF image of IrO_2/GO nanocomposites and (d) the particle size distribution histogram of IrO_2 nanoparticles.

of hydroxyl radicals in the IrO_2/GO–H_2O_2 reaction system [32]. As shown in Fig. 5a, there was no fluorescence of TA

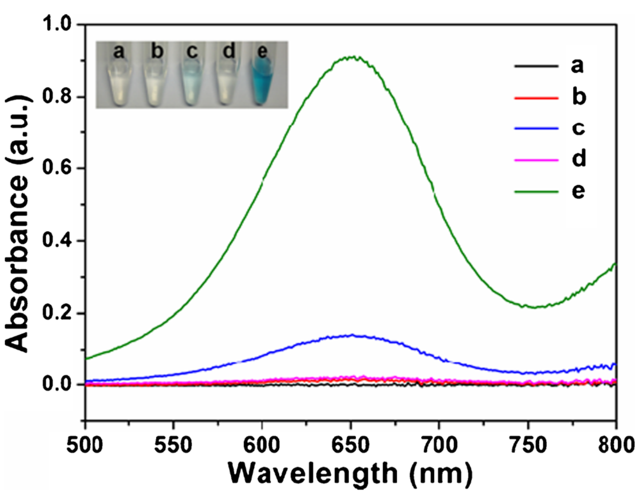

Fig. 3 UV-vis absorption spectra of (a) TMB, (b) TMB + H_2O_2, (c) TMB + GO + H_2O_2, (d) TMB + IrO_2/GO, and (e) TMB + IrO_2/GO + H_2O_2 solution after mixing for 10 min. Inset: the color change of the corresponding solution

without H_2O_2. And the strong fluorescence intensity of TA and H_2O_2 reaction solution at 435 nm implied that the hydroxyl radical can be produced by the intrinsic decomposition of H_2O_2. On the contrary, the fluorescence intensity at 435 nm decreased after IrO_2/GO was added, which indicated that the catalyst was able to quench hydroxyl radical instead of promoting the generation of hydroxyl radical. The experiment results excluded the generation of hydroxyl radical mechanism of peroxidase-like activity of IrO_2/GO nanocomposites.

As an active reactant in the electron transfer process [33, 34], Cyt C was selected to evaluate the electron accepting ability of IrO_2/GO. The absorption spectra of Cyt C with and without IrO_2/GO are presented in Fig. 5b. The two absorption peaks at 520 nm and 550 nm revealed the reduced state of Cyt C (black line), and subsequently disappeared after incubation with IrO_2/GO for 4 h. The oxidized state of Cyt C was confirmed by a new absorption peak at 530 nm (blue line). To eliminate the influence of dissolved oxygen, the solution was bubbled with N_2 for 30 min and incubated with the IrO_2/GO for 4 h in a nitrogen atmosphere. As shown in Fig. 5b, the oxidized state of Cyt C was also obtained in hypoxia

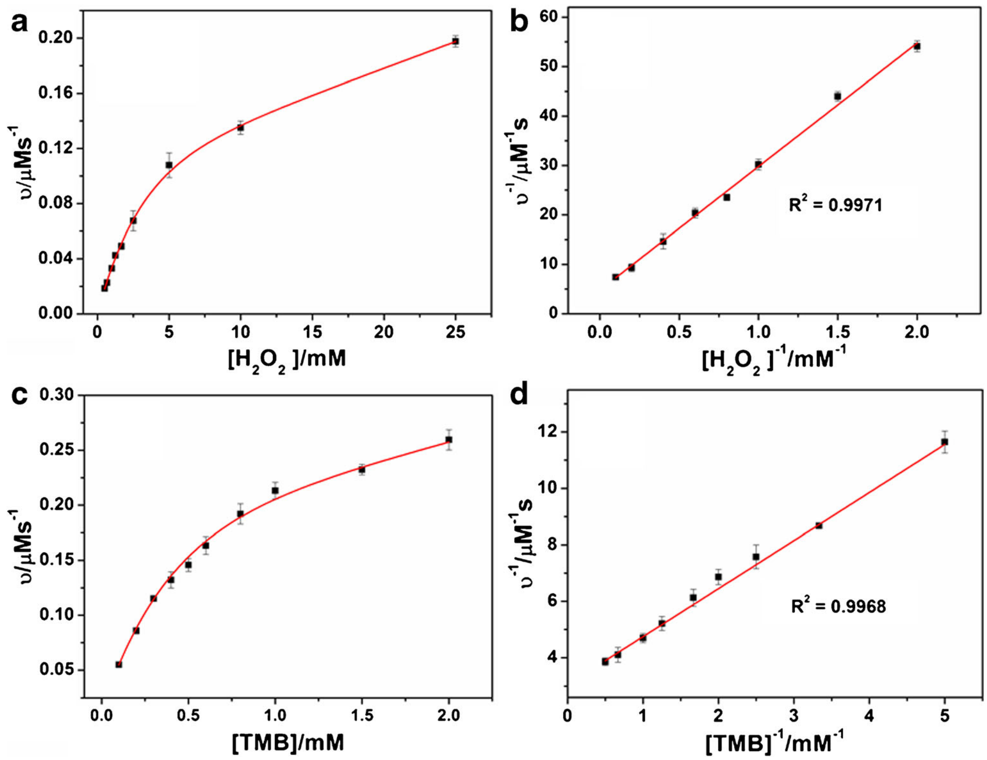

Fig. 4 Steady-state kinetic assay of IrO_2/GO nanocomposites with IrO_2/GO concentration of 2.4 μg·mL^{-1}. (a) and (b) TMB (0.5 mM) with varied concentrations of H_2O_2, (c) and (d) H_2O_2 (5 mM) with varied concentrations of TMB. Analytical wavelength: 652 nm

(red line). The experiment results clearly demonstrated the electron transfer mechanism of peroxidase-like activity of IrO_2/GO nanocomposites.

Colorimetric determination of AA

The IrO_2/GO nanocomposites were applied for colorimetric detection of AA. The detection was conducted with 0.5 mM of TMB, 5 mM of H_2O_2, 5 μL IrO_2/GO dispersion and varied concentrations of AA. As shown in Fig. 6a, the corresponding solution color changed from deep blue to colorless with the increasing concentration of AA, which was clearly visible. In the absorption spectra of the reaction systems with varied concentrations of AA, the absorption peak of ox-TMB at 652 nm decreased as the concentration of AA increased (Fig. 6a). The corresponding absorbance exhibited good linearity to the concentration of AA in the range of 5–70 μM with a coefficient of determination (R^2) equal to 0.9931 (Fig. 6b). The limit of detection (LOD) for AA was estimated to be 324 nM (signal/noise = 3). The kinetics absorbance changes of oxidized TMB at 652 nm with varied concentrations of AA are presented in Fig. S7. As shown in Table S2, this assay exhibits good performance compared to previously reported methods.

For further investigation of the selectivity of the colorimetric detection assay, some other compounds in metabolism like amino acids, carbohydrates and metal ions were selected for test with the same concentration, as presented in Fig. 7. No blue color was observed after adding AA, which was clearly different from the control experiment. However, the color

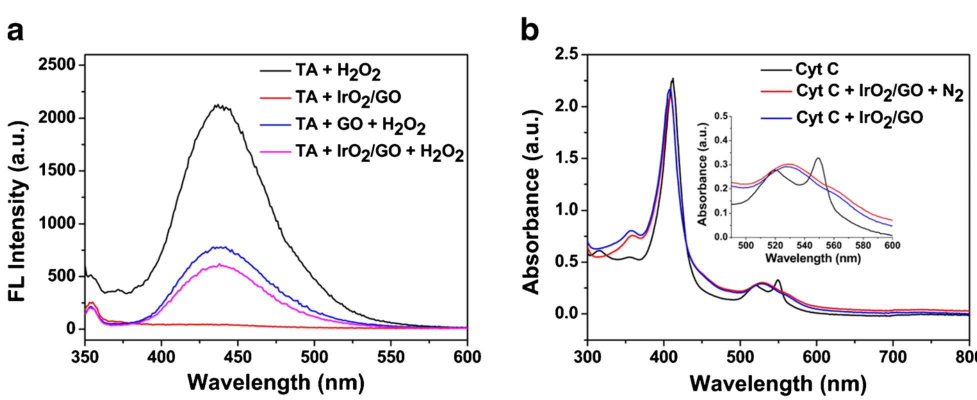

Fig. 5 (a) Fluorescence emission spectra of TA with H_2O_2, TA with IrO_2/GO and TA with both IrO_2/GO and H_2O_2. (b) UV-vis absorption spectra of reduced Cyt C, Cyt C with IrO_2/GO and Cyt C with IrO_2/GO under N_2 atmosphere

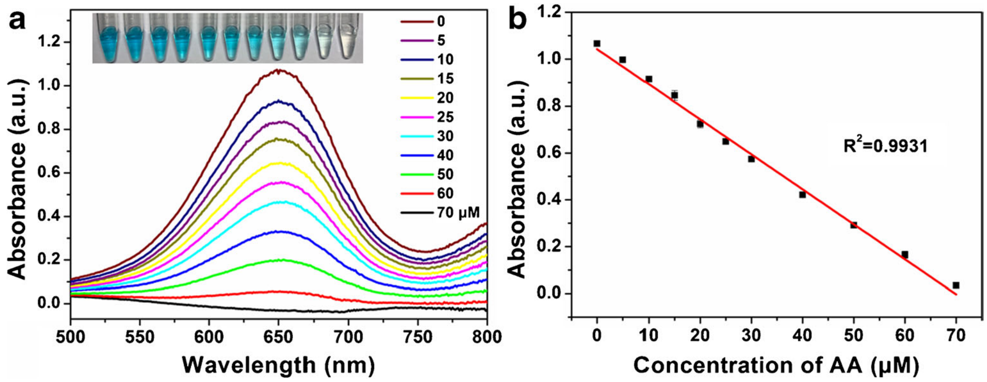

Fig. 6 (a) UV-vis absorption spectra of reaction solutions (TMB 0.5 mM, H_2O_2 5 mM and IrO_2/GO 2.4 μg·mL^{-1}) with different concentrations of AA, inset the corresponding photograph of reaction solutions. (b) The linear calibration plot of absorbance against concentrations of AA after 10 min reaction. Analytical wavelength: 652 nm

changes of solution with other compounds were almost imperceptible compared with the control experiment. The values of absorbance of solution at 652 nm with different substance are also presented in Fig. 7. Compared to the absorbance change with the addition of AA, no obvious inhibition effects were observed after the system was treated with different inferential substrates alone. We noticed that the activity of IrO_2/GO nanozyme was slightly reduced with inorganic salt. However, their effect was far less than that of AA when investigated with the same concentration. The experimental results demonstrated that the colorimetric assay based on IrO_2/GO–H_2O_2–TMB possessed high selectivity for AA.

To further investigate the feasibility of the colorimetric method for detecting AA in real samples, AA concentrations were determined in simulated serum, Vitamin C tablets and Mizone beverage. As listed in Table 1, the experimental results were in good agreement with the specifications, and the recoveries for AA in real samples were in the range of 97.7–103%, indicating that this IrO_2/GO system can be applied for

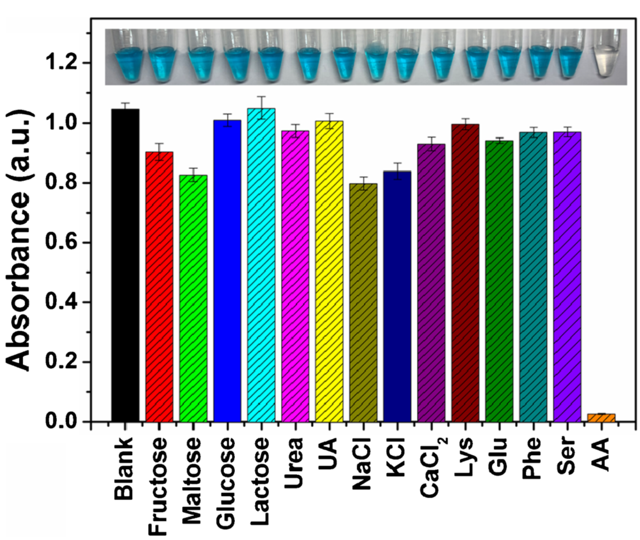

Fig. 7 The selectivity of colorimetric assay for AA detection based on the peroxidase-like activity of IrO_2/GO nanocomposites. The concentration of all interferential substances and AA were 100 μM (inset: the corresponding photographs of reaction solutions). Analytical wavelength: 652 nm

the determination of AA in practical samples. Furthermore, the relative standard deviation (RSD) was within the range of 1.02–1.89%. Although the IrO_2/GO nanozyme has large linear range for detection of AA, its limit of detection is slightly high compared to some other nanomaterials with fluorescence method as shown in Table S2. Taken together, the colorimetric assay based on IrO_2/GO–H_2O_2–TMB was feasible and reliable for detecting AA in real samples.

Conclusion

The IrO_2/GO nanocomposites were successfully synthesized by an environmentally friendly strategy and exhibited high peroxidase-like activity. The following parameters were optimized: pH, temperature, concentrations of H_2O_2 and IrO_2/GO. A colorimetric method for AA detection was developed in the IrO_2/GO–H_2O_2–TMB reaction system. Despite the requirement of constant temperature and pH, the method had the advantage of high accuracy and selectivity and good practicability, which was successfully applied for detecting AA in real samples. Our results indicate that the IrO_2/GO nanocomposites with high peroxidase-like activity will have potential in different applications, such as food safety, environmental monitoring and biomedical diagnosis.

Table 1 Detection of AA in different samples ($n = 3$)

Sample	[a]Concentration of AA (mM)	[b]Experimental results (mM)	Recovery (%)	RSD (%)
BSA	1.0	1.03	103	1.34
	2.5	2.54	101.6	1.89
	5.0	5.03	100.6	1.05
Tablet	60.13	58.76	97.7	1.39
Beverage	1.14	1.16	101.7	1.02

[a] Concentration of AA from the simulated serum, ingredients table of vitamin C tablet and beverage

[b] Results obtained by this work

Analytical wavelength: 652 nm.

Acknowledgments This work was supported by National key research and development program from the Ministry of Science and Technology of China (2016YFC0207102) and National Natural Science Foundation of China (21573050).

Compliance with ethical standards

Conflict of interest The author(s) declare that they have no competing interests.

References

1. Eipper BA, Stoffers DA, Mains RE (1992) The biosynthesis of neuropeptides: peptide alpha amidation. Annu Rev Neurosci 15: 57–85. https://doi.org/10.1146/annurev.ne.15.030192.000421
2. De Rosa S, Cirillo P, Paglia A, Sasso L, Di Palma V, Chiariello M (2010) Reactive oxygen species and antioxidants in the pathophysiology of cardiovascular disease: does the actual knowledge justify a clinical approach? Curr Vasc Pharmacol 8(2):259–275. https://doi.org/10.2174/157016110790887009
3. Moretti M, Budni J, Freitas AE, Rosa PB, Rodrigues AL (2014) Antidepressant-like effect of ascorbic acid is associated with the modulation of mammalian target of rapamycin pathway. J Psychiatr Res 48(1):16–24. https://doi.org/10.1016/j.jpsychires.2013.10.014
4. Malashikhina N, Pavlov V (2012) DNA-decorated nanoparticles as nanosensors for rapid detection of ascorbic acid. Biosens Bioelectron 33(1):241–246. https://doi.org/10.1016/j.bios.2012.01.011
5. Klimczak J, Gliszczyńska-Świgło A (2015) Comparison of UPLC and HPLC methods for determination of vitamin C. Food Chem 175:100–105. https://doi.org/10.1016/j.foodchem.2014.11.104
6. Ma Y, Zhou M, Jin X, Zhang B, Chen H, Guo N (2002) Flow-injection chemiluminescence determination of ascorbic acid by use of the cerium (IV) - Rhodamine B system. Anal Chim Acta 464(2):289–293. https://doi.org/10.1016/S0003-2670(02)00483-X
7. Gao L, Zhuang J, Nie L, Zhang J, Gu N, Wang T, Feng J, Yang D, Perrett S (2007) Intrinsic peroxidase-like activity of ferromagnetic nanoparticles. Nat Nanotechnol 2(9):577–583. https://doi.org/10.1038/nnano.2007.260
8. Primohamed T, Dowding JM, Wasserman B, Heckert E, Karakoti AS, King JE, Seal S, Self WT (2010) Nanoceria exhibit redox state-dependent catalase mimetic activity. Chem Commun 46(16):2736–2738. https://doi.org/10.1039/B922024K
9. Liu X, Wang X, Qi C, Han Q, Xiao W, Cai S, Wang C, Yang R (2019) Sensitive colorimetric detection of ascorbic acid using Pt/CeO_2 nanocomposites as peroxidase mimics. Appl Surf Sci 479: 532–539. https://doi.org/10.1016/j.apsusc.2019.02.135
10. Cui W, Wang Y, Yang D, Du J (2017) Fluorometric determination of ascorbic acid by exploiting its deactivating effect on the oxidase–mimetic properties of cobalt oxyhydroxide nanosheets. Microchim Acta 184(12):4749–4755. https://doi.org/10.1007/s00604-017-2525-4
11. Pedone D, Moglianetti M, De Luca E, Bardi G, Pompa PP (2017) Platinum nanoparticles in nanobiomedicine. Chem Soc Rev 46(16): 4951–4975. https://doi.org/10.1039/c7cs00152e
12. Wu G, He S, Peng H, Deng H, Liu A, Lin X, Xia X, Chen W (2014) Citrate-capped platinum nanoparticle as a smart probe for ultrasensitive mercury sensing. Anal Chem 86(21):10955–10960. https://doi.org/10.1021/ac503544w
13. Liu X, Han Q, Zhang Y, Wang X, Cai S, Wang C, Yang R (2019) Green and facile synthesis of Rh/GO nanocomposites for high catalytic performance. Appl Surf Sci 471:929–934. https://doi.org/10.1016/j.apsusc.2018.12.065
14. Wang S, Deng W, Yang L, Tan Y, Xie Q, Yao S (2017) Copper-based metal-organic framework nanoparticles with peroxidase-like activity for sensitive colorimetric detection of Staphylococcus aureus. ACS Appl Mater Interfaces 9(29):24440–24445. https://doi.org/10.1021/acsami.7b07307
15. Wu T, Hou W, Ma Z, Liu M, Liu X, Zhang Y, Yao S (2019) Colorimetric determination of ascorbic acid and the activity of alkaline phosphatase based on the inhibition of the peroxidase-like activity of citric acid-capped Prussian blue nanocubes. Microchim Acta 186(2):123–129. https://doi.org/10.1007/s00604-018-3224-5
16. Song Y, Qu K, Zhao C, Ren J, Qu X (2010) Graphene oxide: intrinsic peroxidase catalytic activity and its application to glucose detection. Adv Mater 22(19):2206–2210. https://doi.org/10.1002/adma.200903783
17. Chen J, Ge J, Zhang L, Li Z, Li J, Sun Y, Qu L (2016) Reduced graphene oxide nanosheets functionalized with poly(styrene sulfonate) as a peroxidase mimetic in a colorimetric assay for ascorbic acid. Microchim Acta 183(6):1847–1853. https://doi.org/10.1007/s00604-016-1826-3
18. Othman A, Karimi A, Andreescu S (2016) Functional nanostructures for enzyme based biosensors: properties, fabrication and applications. J Mater Chem B 4(45):7178–7203. https://doi.org/10.1039/c6tb02009g
19. Amendola V, Meneghetti M (2009) Laser ablation synthesis in solution and size manipulation of noble metal nanoparticles. Phys Chem Chem Phys 11(20):3805–3821. https://doi.org/10.1039/b900654k
20. Jenck JF, Agterberg F, Droescher MJ (2004) Products and processes for a sustainable chemical industry: a review of achievements and prospects. Green Chem 6(11):544–556. https://doi.org/10.1039/b406854h
21. Zhang D, Gökce B, Barcikowski S (2017) Laser synthesis and processing of colloids: fundamentals and applications. Chem Rev 117(5):3990–4103. https://doi.org/10.1021/acs.chemrev.6b00468
22. Zhang J, Chaker M, Ma D (2016) Pulsed laser ablation based synthesis of colloidal metal nanoparticles for catalytic applications. J Colloid Interface Sci 489:138–149. https://doi.org/10.1016/j.jcis.2016.07.050
23. Wagener P, Schwenke A, Barcikowski S (2012) How citrate ligands affect nanoparticle adsorption to microparticle supports. Langmuir 28(14):6132–6140. https://doi.org/10.1021/la204839m
24. Zhang J, Chen G, Chaker M, Rosei F, Ma D (2013) Gold nanoparticle decorated ceria nanotubes with significantly high catalytic activity for the reduction of nitrophenol and mechanism study. Appl Catal B-Environ 132:107–115. https://doi.org/10.1016/j.apcatb.2012.11.030
25. Reina G, Gonzálezdomínguez JM, Criado A, Vázquez E, Bianco A, Prato M (2017) Promises, facts and challenges for graphene in biomedical applications. Chem Soc Rev 46(15):4400–4416. https://doi.org/10.1039/c7cs00363c
26. Sun M, Wang Q, Zou J, Zhang X (2013) Research progress of IrO_2 as electrode materials. Electroplat & Finishing 32(10):54–59. https://doi.org/10.3969/j.issn.1004-227X.2013.10.014
27. Zhang D, Gökce B, Barcikowski S (2017) Laser synthesis and processing of colloids: fundamentals and applications. Chem Rev 117(5):3990–4103. https://doi.org/10.1021/acs.chemrev.6b00468
28. Kwak I, Kwon IS, Kim J, Park K, Ahn JP, Yoo SJ, Kim JG, Park J (2017) IrO_2–ZnO hybrid nanoparticles as highly efficient trifunctional electrocatalysts. J Phys Chem C 121(27):14899–14906. https://doi.org/10.1021/acs.jpcc.7b03844
29. Kötz R, Neff H, Stucki S (1984) Anodic iridium oxide films: XPS-studies of oxidation state changes and O_2 evolution. J Electrochem Soc 131(1):72–77. https://doi.org/10.1149/1.2115548

30. Cui M, Zhou J, Zhao Y, Song Q (2017) Facile synthesis of iridium nanoparticles with superior peroxidase-like activity for colorimetric determination of H_2O_2 and xanthine. Sensor Actuat B-Chem 243: 203–210. https://doi.org/10.1016/j.snb.2016.11.145
31. Liu Y, Yu F (2011) Substrate-specific modifications on magnetic iron oxide nanoparticles as an artificial peroxidase for improving sensitivity in glucose detection. Nanotechnology 22(14):145704–145711. https://doi.org/10.1088/0957-4484/22/14/145704
32. Mu J, Wang Y, Zhao M, Zhang L (2012) Intrinsic peroxidase-like activity and catalase-like activity of Co_3O_4 nanoparticles. Chem Commun 48(19):2540–2542. https://doi.org/10.1039/c2cc17013b
33. Dong J, Song L, Yin J, He W, Wu Y, Gu N, Zhang Y (2014) Co_3O_4 nanoparticles with multi-enzyme activities and their application in Immunohistochemical assay. ACS Appl Mater Interfaces 6(3): 1959–1970. https://doi.org/10.1021/am405009f
34. Su H, Liu D, Zhao M, Hu W, Xue S, Cao Q, Le X, Ji L, Mao Z (2015) Dual-enzyme characteristics of Polyvinylpyrrolidone-capped iridium nanoparticles and their cellular protective effect against H_2O_2-induced oxidative damage. ACS Appl Mater Interfaces 7(15):8233–8242. https://doi.org/10.1021/acsami.5b01271